Two-dimensional photoelectron momentum distribution of hydrogen in intense laser field*

Sun Chang-Ping(孙长平)[a)], Zhao Song-Feng(赵松峰)[a)],
Chen Jian-Hong(陈建宏)[a)b)], and Zhou Xiao-Xin(周效信)[a)†]

[a)] *Key Laboratory of Atomic and Molecular Physics and Functional Materials of Gansu Province, College of Physics and Electronic Engineering, Northwest Normal University, Lanzhou* 730070, *China*
[b)] *Peili College of Engineering and Technique, Lanzhou City University, Lanzhou* 730070, *China*

(Received 20 January 2011; revised manuscript received 24 March 2011)

Two-dimensional (2D) electron momentum distributions and energy spectra of a hydrogen in an intense laser field are calculated by solving the time-dependent Schrödinger equation combined with the window-operator technique. Compared with the standard projection technique, the window-operator technique has the advantage that the continuum states of atoms can be avoided in the calculation. We show that the 2D electron momentum distributions and the energy spectra from those two techniques accord quite well with each other if an appropriate energy width is used in the window operator.

Keywords: momentum distribution, energy spectra, time-dependent Schrödinger equation

PACS: 32.80.Rm, 32.80.Fb, 42.50.Hz **DOI:** 10.1088/1674-1056/20/11/113201

1. Introduction

In recent years, the two-dimensional (2D) electron momentum distributions and the energy spectra of atoms have been extensively investigated both experimentally and theoretically.[1−12] More importantly, based on the recently developed quantitative rescattering (QRS) theory,[7−9] accurate electron–atom elastic scattering cross sections can be directly retrieved from the high-energy 2D momentum spectra of atoms in the laser field.[7−9,13]

Theoretically, the 2D electron momentum distributions and the energy spectra can be calculated with the strong-field approximation (SFA).[9,14] The limitation of the SFA is known. For the high-energy above-threshold-ionization (HATI) spectra, the QRS theory can give more accurate results than the SFA.[8] To seriously compare the experimental results, more elaborate calculations, such as the numerical solution of the time-dependent Schrödinger equation (TDSE), are needed.[15] The standard technique for calculating the 2D electron momentum distributions and the energy spectra is that the final wavefunction is projected onto the continuum eigenstates of the unperturbed Hamiltonian, which will be called the projection technique (PT) in the following. Obtaining numerical solutions for the TDSE is rather time-consuming, especially for the longer wavelength. To avoid the explicit calculations of the continuum eigenstates of the atoms, an implicit window-operator technique (WOT) was proposed.[16] In Ref. [16], the above-threshold-ionization (ATI) spectra and the energy-resolved angular distribution of a hydrogen were presented for a fixed energy width γ with order of the window operator $n = 2$. Recently, Bauer[17] studied the effect of width γ on the energy spectra using higher order of the window operator $n = 3$. As far as we know, there have not been any investigations of the 2D momentum distribution for the hydrogen atom with the WOT. In this paper, the validity of the window-operator technique is carefully examined by comparing the 2D momentum distributions and the energy spectra of the hydrogen atom obtained from the WOT and from the standard projection technique. Atomic units (a.u.) are used throughout in the paper unless otherwise indicated.

*Project supported by the National Natural Science Foundation of China (Grant Nos. 11044007 and 11064013), the Specialized Research Fund for the Doctoral Program of Higher Education of China (Grant No. 20096203110001), and the Foundation of Northwest Normal University, China (Grant Nos. NWNU-KJCXGC-03-62 and NWNU-KJCXGC-03-70).

†Corresponding author. E-mail: zhouxx@nwnu.edu.cn

© 2011 Chinese Physical Society and IOP Publishing Ltd

2. Theoretical method

The details of the projection technique have been given in Refs. [18] and [19]. Here, we briefly review the window-operator technique.[16,17] Based on the single-active-electron (SAE) approximation and in the velocity gauge, the TDSE of a hydrogen in the presence of a linearly polarized laser field can be expressed as

$$\mathrm{i}\frac{\partial\Psi(\boldsymbol{r},t)}{\partial t}=H(t)\Psi(\boldsymbol{r},t), \tag{1}$$

where

$$H(t)=\frac{1}{2}\left[\hat{\boldsymbol{p}}+\boldsymbol{A}(t)\right]^2-\frac{1}{r}, \tag{2}$$

with $\boldsymbol{A}(t)$ being the vector potential of the laser field and $\hat{\boldsymbol{p}}$ the moment operator. The wavefunction $\Psi(\boldsymbol{r},t)$ of the hydrogen can be expanded as

$$\Psi(\boldsymbol{r},t)=\frac{1}{r}\sum_{l=0}^{L-1}R_{l0}(r,t)\mathrm{Y}_{l0}(\Omega), \tag{3}$$

where R is the radial wavefunction, Y is the spherical harmonic function, Ω is the solid angle, and L is the maximum number of the partial waves. Equation (1) can be solved by using the split-operator method with the box of $r\in[0,r_{\max}]$.

In order to avoid the explicit calculation of the continuum wavefunction, a window operator W_γ is defined as

$$W_\gamma=\frac{\gamma^{2n}}{(\hat{H}_0-\varepsilon)^{2n}+\gamma^{2n}}, \tag{4}$$

where ε is the energy, γ is the energy width, n is the integer order of the window operator ($n=3$ is used in the present calculations), and $\hat{H}_0$ is the unperturbed Hamiltonian of the hydrogen atom.

Once the final wavefunction $\Psi_{\mathrm{f}}=\Psi(\boldsymbol{r},t=t_{\mathrm{f}})$ is obtained, the energy component $|\Phi_\gamma(\varepsilon)\rangle$ of Ψ_{f} within the bin of width 2γ centred at ε can be calculated as

$$|\Phi_\gamma(\varepsilon)\rangle=\hat{W}_\gamma(\varepsilon)\,|\Psi_{\mathrm{f}}\rangle\,. \tag{5}$$

Within the energy bin of width 2γ centred around ε and with order n, the probability $P_\gamma(\varepsilon)$, with which an electron is found in the final state, is given by

$$\begin{aligned}P_\gamma(\varepsilon)&=\langle\Psi_{\mathrm{f}}|\,\hat{W}_\gamma^2(\varepsilon)\,|\Psi_{\mathrm{f}}\rangle\\&=\langle\Phi_\gamma(\varepsilon)\,|\Phi_\gamma(\varepsilon)\rangle\\&=\sum_j|\langle\Psi_{\mathrm{f}}|\,j\rangle|^2f_j(\gamma,n),\end{aligned} \tag{6}$$

where $|j\rangle$ and ε_j are the eigenvector and the eigenvalue of $\hat{H}_0$, respectively. The shape function takes the form

$$f_j(\gamma,n)=\left[\frac{\gamma^{2n}}{(\varepsilon_j-\varepsilon)^{2n}+\gamma^{2n}}\right]^2. \tag{7}$$

The quantum distribution function $P_\gamma(\varepsilon,\Omega,r)$ in the energy and position space is given by

$$\begin{aligned}&P_\gamma(\varepsilon,\Omega,r)\\&=\sum_{ll'}\mathrm{Y}^*_{l'0}(\Omega)\mathrm{Y}_{l0}(\Omega)R_{l'}^{(\Phi_\gamma)^*}(r)R_l^{(\Phi_\gamma)}(r).\end{aligned} \tag{8}$$

Due to the cylindrical symmetry of the atom in the case of the linearly polarized pulse, the 2D momentum distribution of the hydrogen can be calculated as

$$\begin{aligned}\frac{\partial^2P}{\partial E\partial\theta}&=P_\gamma\left(\varepsilon,\theta\right)\\&=\int\mathrm{d}\varphi\int\mathrm{d}rP_\gamma(\varepsilon,\Omega,r)\sin\theta\\&=\int\mathrm{d}\varphi\int\mathrm{d}r\left|\sum_l R_{l0}^{(\Phi_\gamma)}\left(r\right)\mathrm{Y}_{l0}\left(\Omega\right)\right|^2\sin\theta,\end{aligned} \tag{9}$$

where E is the kinetic energy of the detached electron, and θ is the angle between the polarization axis of the laser field and the direction of the ejected photoelectron. The energy spectra are given by

$$\begin{aligned}\frac{\partial P}{\partial E}&=P_\gamma\left(\varepsilon\right)\\&=\int\mathrm{d}\theta P_\gamma(\varepsilon,\theta)\\&=\sum_l\int\mathrm{d}rR_{l0}^{(\Phi_\gamma)^*}\left(r\right)R_{l0}\left(r\right).\end{aligned} \tag{10}$$

3. Results and discussion

We solve the TDSE of the hydrogen in the velocity gauge with the QPROP packet,[20] and then the window-operator technique is used to obtain the 2D momentum distributions and the energy spectra. The $L=45$ and $r_{\max}=6000$ a.u. are used in our present calculations. To quantitatively examine the window-operator technique, the 2D momentum distributions and the energy spectra are also calculated by solving the TDSE of the hydrogen in the length gauge together with the projection technique,[8,9,18] in which $L=120$ and $r_{\max}=1000$ a.u. are used.

For a linearly polarized laser pulse (along the z axis), the electric field is taking the form

$$\boldsymbol{E}(t)=\widehat{\boldsymbol{z}}E_0\cos^2\left(\frac{\pi t}{\tau}\right)\cos(\omega t+\phi) \tag{11}$$

for the time interval $(-\tau/2,\tau/2)$ and is zero elsewhere. Here ω is the carrier frequency, carrier-envelope phase (CEP) ϕ is set as 0 rad, and the pulse duration is

$\tau = 5T$, with T being the optical cycle of the laser pulse.

The 2D momentum distributions and the energy spectra obtained from the WOT are normalized to those from the PT in this paper. Figure 1 shows the electron energy spectra of the hydrogen with a laser intensity of 1×10^{14} W/cm^2 and a laser wavelength of 800 nm. The corresponding Keldysh parameter[21] is $\eta = 1.07$. The energy spectrum from the WOT is normalized to that from the PT near the cut-off. The normalization factor is 60. In Fig. 1, we can clearly see that the energy spectra from these two methods accord quite well with each other.

The 2D electron momentum distributions of the hydrogen are shown in Fig. 2. Again, the results from the WOT are normalized to those from the PT with the factor 60. In Fig. 2, the horizontal axis is along the laser polarization direction, and the vertical axis is any direction perpendicular to it. In Figs. 2(a) and 2(c), the consistence between these two methods is also good. The ubiquitous fanlike structures are observed in the low-energy 2D momentum spectra, which have been well explained in Ref. [22]. As the electron yield decreases very rapidly with the energy increasing (see Fig. 1), to make the high-energy part readily visible, the 2D momentum distributions in each frame have been renormalized so that the total ionization yield at each electron energy is the same. The high-energy 2D momentum spectra from these two methods also stay essentially the same, as shown in Figs. 2(b) and 2(d). In the high-energy region, there are two outmost half circular rings called the back rescattered ridges (BRR),[23] which represent electrons that have been rescattered into the backward directions by the parent ion, one on the left and the other on the right (see Figs. 2(b) and 2(d)).

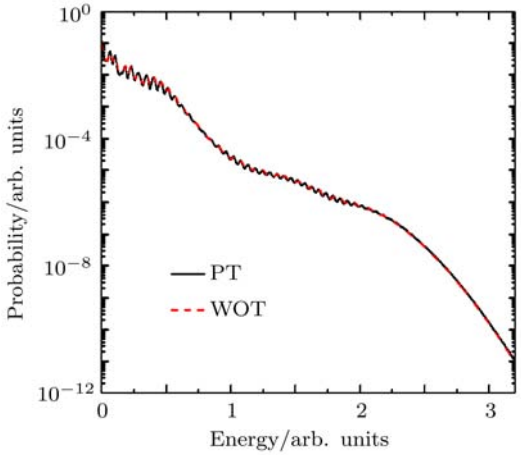


Fig. 1. (colour online) Electron energy spectra of atomic hydrogen in a five-cycle laser pulse with a wavelength of 800 nm and a peak intensity of 1×10^{14} W/cm^2. The $\gamma = 0.01$ is used in the WOT.

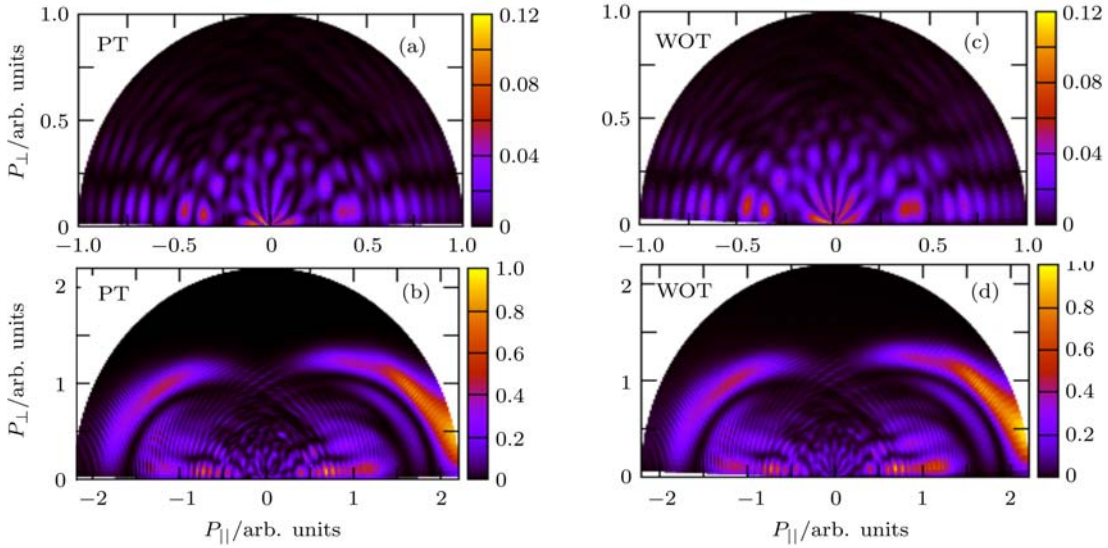


Fig. 2. (colour online) The 2D electron momentum distributions of hydrogen atom. Panels (a) and (b) show the results calculated using the PT, panels (c) and (d) show the results obtained from the WOT with $\gamma = 0.01$. Note that panels (b) and (d) show the renormalized results. The laser parameters are the same as those in Fig. 1.

To quantitatively compare the high-energy 2D momentum distribution from the WOT with that from the PT, we extract from Figs. 2(b) and 2(d) the electron yields along the right BRR with radius $p_r = 1.19$ centred at $A_r = 0.92$ and compare them with the e–H elastic differential scattering cross sections. For the hydrogen, the elastic differential cross section (DCS) can be given by the Rutherford formula. In Fig. 3, we

focus on scattering angle $\theta_r > 100°$ only. We can see that the electron yields along the BRR from these two methods are very close to the elastic DCS (normalized), which indicates that the elastic DCS of the electrons can be directly extracted from the high-energy 2D momentum distribution.

To further examine the validity of the window-operator technique, we show the 2D momentum spectra of the hydrogen atom at wavelengths of 400 nm, 600 nm, and 1000 nm in Fig. 4. To fix the Keldysh parameter at 1.07, the corresponding laser intensities of 4×10^{14} W/cm^2, 1.78×10^{14} W/cm^2, and 6.4×10^{13} W/cm^2 are used, respectively. For these three different wavelengths, the same factor 60 is used to normalize the results of the WOT to those from the PT. To compare the high-energy part, the renormalized 2D momentum distributions are also shown in Fig. 5. The good agreement of the 2D momentum spectra between these two methods indicates that the WOT works well for these wavelengths (see Figs. 4 and 5).

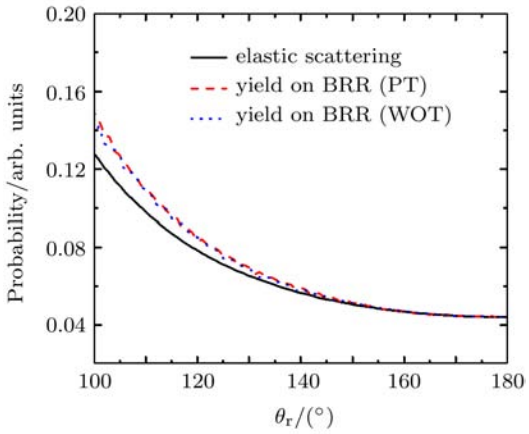


Fig. 3. (colour online). Angular distributions of photoelectrons along the BRR compared with the elastic differential cross section for the H target ion. The BRRs are taken to be the outmost half circles on the right side of Figs. 2(b) and 2(d) respectively.

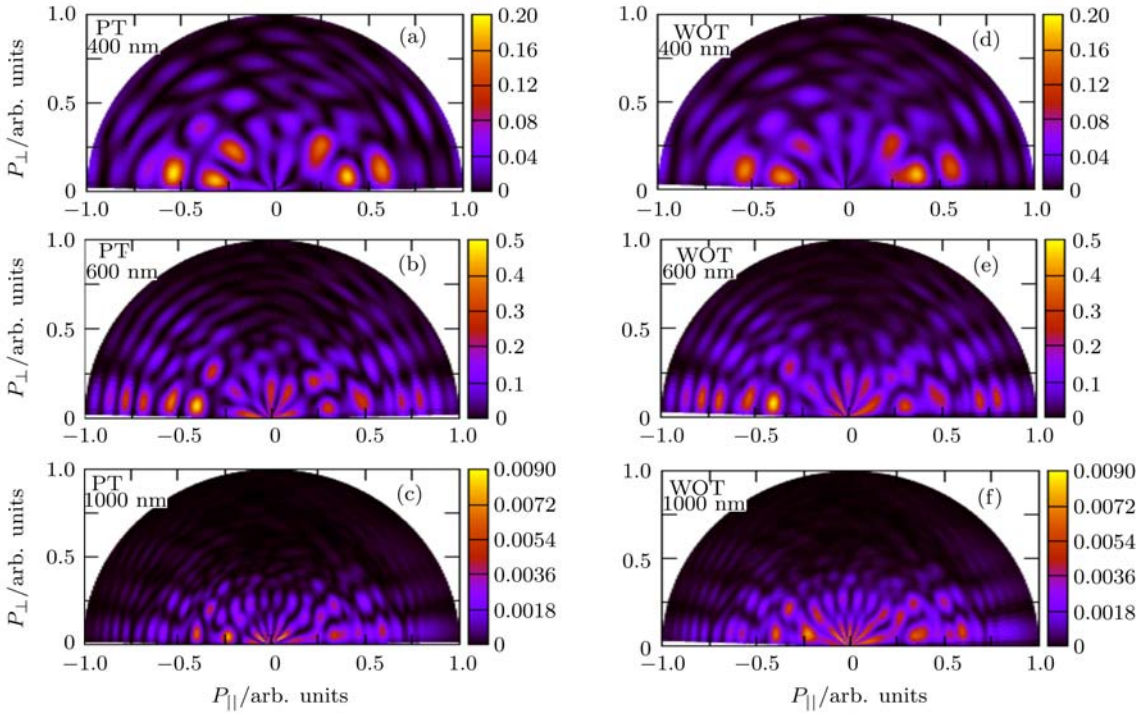


Fig. 4. (colour online) The 2D momentum distributions of atomic hydrogen with wavelengths of 400 nm, 600 nm, and 1000 nm (from top to bottom). Panels (a), (b), and (c) show the results calculated by the PT; panels (d), (e), and (f) exhibit the results obtained from the WOT ($\gamma = 0.01$).

We mention that energy width $\gamma = 0.01$ is used in the above WOT calculations. Since quantum distribution function $P_\gamma(\varepsilon, \Omega, r)$ depends on energy width γ, it is essential to study the effect of energy width γ on the 2D electron momentum distributions and the energy spectra. Figure 6 shows the electron energy spectra of the hydrogen obtained from the WOT with three different γ values: 0.002, 0.01 and 0.04. The energy spectrum from the PT is also given for comparison. Note that the energy spectra obtained from the WOT are normalized to that from the PT near the cut-off with the normalization factors of 300, 60, and 15 for γ values of 0.002, 0.01, and 0.04, respectively. In Fig. 6, we can clearly see that the agreement between the energy spectra obtained from these two methods becomes better as γ decreases, which is due

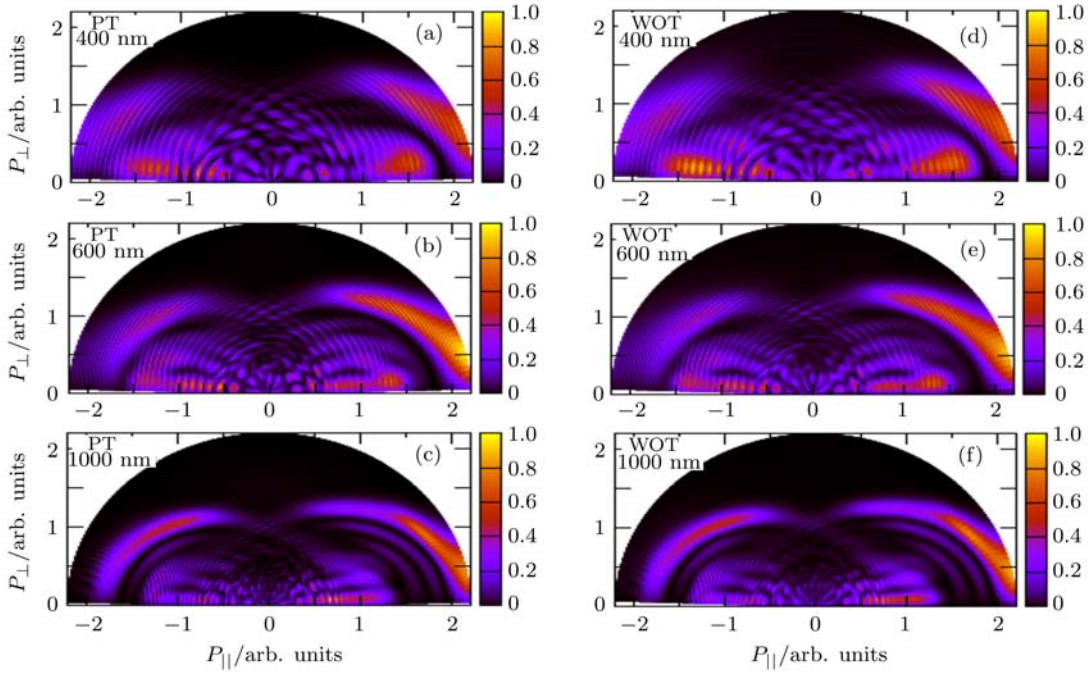


Fig. 5. (colour online) Renormalized 2D momentum distributions of atomic hydrogen. Laser parameters are the same as those in Fig. 4. Panels (a), (b) and (c) show the results from the PT; panels (d), (e) and (f) show the results from the WOT.

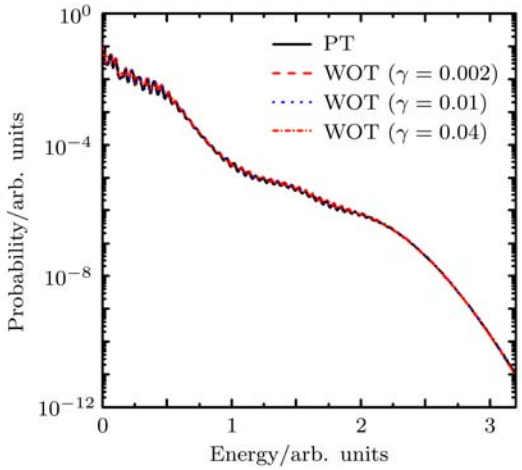


Fig. 6. (colour online) Comparisons between electron energy spectra obtained from the PT and the WOT with three different γ values. The laser parameters are the same as those in Fig. 1.

to the different energy resolutions and is in consistence with the prediction in Ref. [17]. Thus energy width γ is a crucial adjustable parameter to obtain the highly accurate results in the WOT calculation. In Fig. 7, we compare the 2D electron momentum distributions of the hydrogen calculated by these two methods. The electron momentum distributions obtained from the WOT with γ values of 0.002 and 0.01 are in good agreement with those from the PT, while a large discrepancy can be seen in the low-energy region in the comparison of the results obtained from the WOT with a larger γ value (0.04) and from the PT. Figure 8 shows the renormalized 2D electron momentum distributions of the hydrogen. By comparison with the standard PT result, we find a small discrepancy along the BRR for the γ value of 0.002. Thus, based on the calculation of the TDSE with the WOT, we find that at a larger energy width ($\gamma = 0.04$), the poor energy resolutions are obtained in the energy spectra (Fig. 6) and the 2D electron momentum distributions (Figs. 7 and 8). In the case of $\gamma = 0.002$, the low-energy electron momentum spectra accord well with those obtained from the PT (Figs. 7(a) and 7(c)), while small differences do exist in the high-energy region (Figs. 8(a) and 8(c)). In addition, our calculations show that by using the optimized energy width ($\gamma = 0.01$), a quite good agreement between these two methods can be achieved.

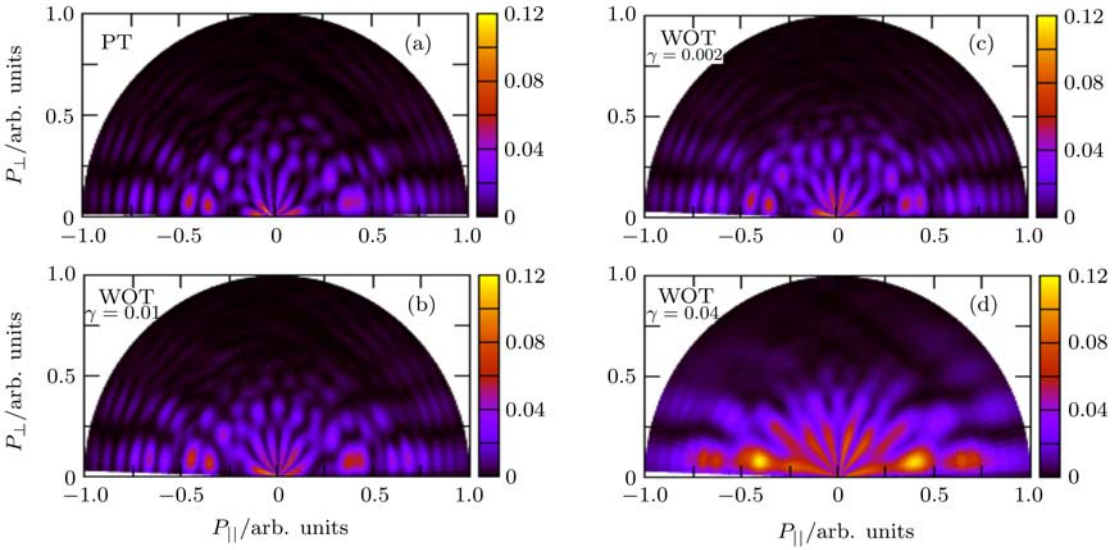


Fig. 7. (colour online) Comparisons between the 2D momentum distributions of hydrogen atom obtained from the PT (a), and the WOT ((b)–(d)) with γ values of 0.01, 0.002 and 0.04, respectively. The laser parameters are the same as those in Fig. 1.

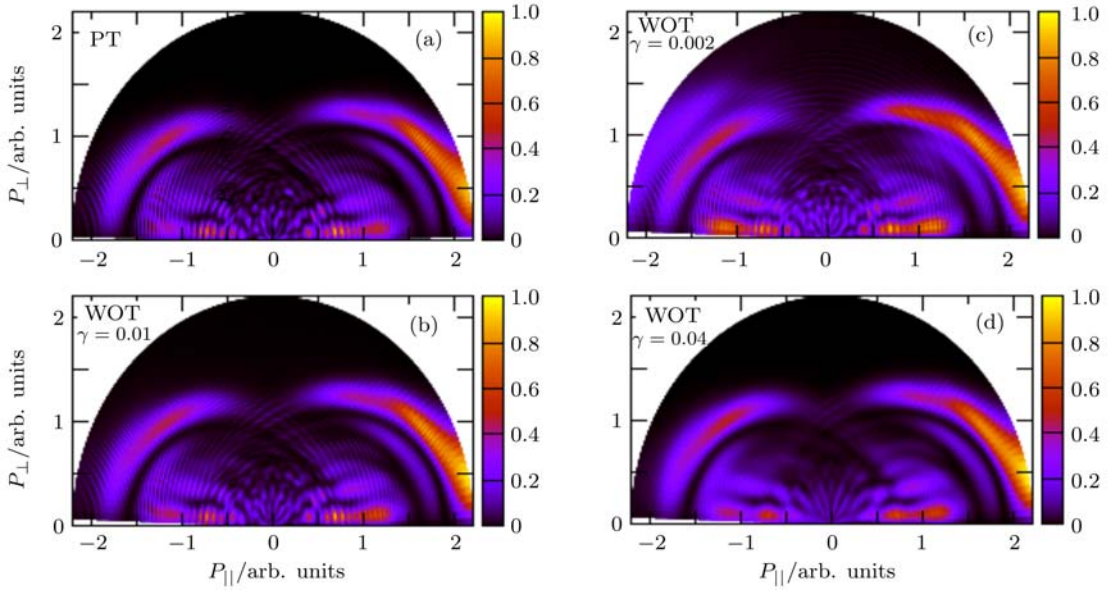


Fig. 8. (colour online) Renormalized 2D momentum distributions of atomic hydrogen obtained from the PT (a) and the WOT ((b)–(d)). Laser parameters are the same as those given in Fig. 7.

4. Conclusion

In this paper, by comparison with the standard projection technique, we carefully establish the validity of the window-operator technique for the investigation of the energy spectra and the 2D electron momentum distributions of the hydrogen atom in an infrared laser field. We demonstrate that the continuum eigenstates of the unperturbed Hamiltonian needed in the PT can be avoided in the calculation with the WOT. This advantage can efficiently reduce the computational time, especially for the case of a longer wavelength. By using the optimized energy width ($\gamma = 0.01$) in the WOT, the electron energy spectra and the 2D electron momentum distributions accord quite well with those from the PT. Hopefully, the WOT can be extended to the study of the above-threshold ionization of molecules in the futures.

References

[1] Yang B, Schafer K J, Walker B, Kulander K C, Agostini P and DiMauro L F 1993 *Phys. Rev. Lett.* **71** 3770

[2] Paulus G G, Nicklich W, Xu H, Lambropoulos P and Walther H 1994 *Phys. Rev. Lett.* **72** 2851
[3] Gaarde M B, Schafer K J, Kulander K C, Sheehy B, Kim D and DiMauro L F 2000 *Phys. Rev. Lett.* **84** 2822
[4] Rudenko A, Zrost K, Schröter C D, de Jesus V L B, Feuerstein B, Moshammer R and Ullrich J 2004 *J. Phys.* B **37** L407
[5] Maharjan C M, Alnaser A S, Litvinyuk I, Ranitovic P and Cocke C L 2006 *J. Phys.* B **39** 1955
[6] Milošević D B, Paulus G G, Bauer D and Becker W 2006 *J. Phys.* B **39** R203
[7] Lin C D, Le A T, Chen Z, Morishita T and Lucchese R R 2010 *J. Phys.* B **43** 122001
[8] Morishita T, Le A T, Chen Z and Lin C D 2008 *Phys. Rev. Lett.* **100** 013903
[9] Chen Z, Le A T, Morishita T and Lin C D 2009 *Phys. Rev.* A **79** 033409
[10] Muller H G and Kooiman F C 1998 *Phys. Rev. Lett.* **81** 1207
[11] Chen B Z 2000 *Chin. Phys.* **9** 351
[12] Chen B Z 1998 *Acta Phys. Sin.* (Overseas edition) **7** 817
[13] Morishita T, Okunishi M, Shimada K, Prumper G, Chen Z J, Watanabe S, Ueda K and Lin C D 2009 *J. Phys.* B **42** 105205
[14] Milošević D B, Hasović E, Busuladžić M, Gazibegović Busuladžić A and Becker W 2007 *Phys. Rev.* A **76** 053410
[15] Morishita T, Chen Z, Watanabe S and Lin C D 2007 *Phys. Rev.* A **75** 023407
[16] Schafer K J and Kulander K C 1990 *Phys. Rev.* A **42** 5794
[17] Bauer D 2005 *Phys. Rev. Lett.* **94** 113001
[18] Chen Z, Morishita T, Le A T, Wickenhauser M, Tong X M and Lin C D 2006 *Phys. Rev.* A **74** 053405
[19] Peng L Y, Pronin E A and Starace A F 2008 *New J. Phys.* **10** 025030
[20] Bauer D and Koval P 2006 *Comp. Phys. Commun.* **174** 396
[21] Keldysh L V 1964 *Sov. Phys. JETP* **20** 1307
[22] Chen Z, Morishita T, Le A T, Wickenhauser M, Tong X M and Lin C D 2006 *Phys. Rev.* A **74** 053405
[23] Chen Z, Morishita T, Le A T and Lin C D 2007 *Phys. Rev.* A **76** 043402